

# Transfer RNA–Pseudouridine Synthetase Pus1 of *Saccharomyces cerevisiae* Contains One Atom of Zinc Essential for Its Native Conformation and tRNA Recognition<sup>†</sup>

Véronique Arluison,<sup>‡</sup> Codjo Hountondji,<sup>§</sup> Bruno Robert,<sup>||</sup> and Henri Grosjean<sup>\*,‡</sup>

CNRS, Laboratoire d'Enzymologie et Biochimie Structurales; 1, avenue de la Terrasse, 91198 Gif-sur-Yvette cedex, France, Laboratoire de Biochimie, URA CNRS 1970, Ecole Polytechnique, 91128 Palaiseau cedex, France and SBPM, DBCM/CEA, URA 2096, 91191 C.E. Saclay, France

Received October 28, 1997; Revised Manuscript Received February 9, 1998

**ABSTRACT:** RNA:pseudouridine synthetase (Pus1) from *Saccharomyces cerevisiae* is a multisite specific enzyme that catalyzes the formation of pseudouridine at positions 34 and 36 of intron-containing precursor tRNA<sup>le</sup> and at positions 27 and/or 28 of several yeast tRNAs. In this paper we demonstrate that the purified recombinant Pus1, expressed in *Escherichia coli*, contains one atom of zinc per 63-kDa monomer, as determined by atomic absorption spectroscopy. This zinc ion could not be removed by treatment with EDTA or urea. However, a zinc-depleted enzyme was obtained after prolonged dialysis against the specific chelating agent 1,10-phenanthroline. Removal of the zinc ion resulted in inactivation of the enzyme with concomitant loss of its ability to bind tRNA. Dialysis of the zinc-depleted inactive enzyme against buffer containing zinc ions led to recovery of up to 25% of bound zinc in parallel with 25% of its initial activity. Removal of the tightly bound zinc atom resulted in a conformational change of the protein, as determined by analytical ultracentrifugation, with minor changes in the internal structure of the protein, as evidenced by circular dichroism and infrared and fluorescence spectroscopy. Our results are consistent with a structural role for the zinc in the tRNA–pseudouridine synthetase Pus1; zinc ion could maintain the association between domains structurally organized around the coordinated metal ion. Zinc chelation was never demonstrated for any of the tRNA–pseudouridine synthetases characterized so far.

Pseudouridine, an isomer of uridine [5-( $\beta$ -D-ribofuranosyl)uracil, abbreviated  $\Psi$ ], is the most abundant modified nucleoside found in all cellular RNAs.<sup>1</sup> For example, among the different cytoplasmic tRNAs,  $\Psi$  can occur at 26 different positions (1, 2). In small nuclear RNAs (snRNA), the number of  $\Psi$ s observed is also high (up to 10%) (3, 4, 5). In ribosomal RNAs,  $\Psi$ s are found in the small or large subunit of the ribosome, most of them being clustered in the conserved domains of the molecule (6).

Several distinct enzymes have been shown to catalyze the formation of  $\Psi$  during the complex process of RNA maturation. In yeast tRNAs,  $\Psi_{13}$ ,  $\Psi_{32}$ , and  $\Psi_{55}$  are formed by distinct site-specific pseudouridine synthetases (7, 8), while the formation of  $\Psi_{27}$ ,  $\Psi_{34}$ , and  $\Psi_{36}$  as well as  $\Psi_{38}$  and  $\Psi_{39}$  is catalyzed by two distinct multisite, specific

tRNA– $\Psi$  synthetases, namely Pus1 and Pus3 (9, 10). The formation of the different  $\Psi$  in eukaryotic snRNA also appears to be catalyzed by distinct enzymes (11, 12), but none of them have been yet purified. In *Escherichia coli*, the most extensively studied pseudouridine synthetase is TruA (also called *hisT* gene product or PSU-I) (13). It catalyzes the formation of  $\Psi$  at positions 38, 39, and 40 in tRNAs. The protein TruB, which catalyzes the formation of  $\Psi$  at position 55 in tRNAs (14), as well as two distinct rRNA– $\Psi$  synthetases (RsuA and RluA) have also been characterized in *E. coli*. RsuA and RluA catalyze the formation of  $\Psi_{516}$  in 16S rRNA within a ribonucleoprotein complex (15) and of  $\Psi_{746}$  in 23S rRNA (16), respectively. RluA catalyzes in vitro the formation of  $\Psi$  in two types of RNA (dual specificity), namely the 23S rRNA ( $\Psi_{746}$ ) and the tRNA ( $\Psi_{32}$ ).

RNA–pseudouridine synthetases catalyze pseudouridine formation only on RNA macromolecules and apparently do not require any cofactor or external source of energy. The molecular mechanism used by pseudouridine synthetases is not yet elucidated. It is proposed that these enzymes cleave the N-glycosidic bond of the targeted uridines and rotate the uracil base by 180°, thus creating a new glycosidyl C–C bond involving the C5 atom of uracil. During catalysis, the hydrogen atom originally bonded to C5 is released as a proton. This latter property has been used to develop an in vitro assay using tRNA harboring radioactive 5-<sup>3</sup>H-uracil (17).

<sup>†</sup> This work was supported by grants from the Centre National de la Recherche Scientifique (ACC-5 program) and from the "Action pour la Recherche sur le Cancer" (ARC, 1997–1998).

\* To whom correspondence should be addressed. E-mail: Henri.Grosjean@lebs.cnrs-gif.fr. Fax: 33-1 69 82 31 29.

<sup>‡</sup> Laboratoire d'Enzymologie et Biochimie Structurales.

<sup>§</sup> Laboratoire de Biochimie.

<sup>||</sup> SBPM, DBCM/CEA.

<sup>1</sup> Abbreviations: BSA, bovine serum albumin; DEP, diethyl pyrocarbonate; DDM, dodecyl-D-maltoside; DTNB, 5,5'-dithio-bis(2-nitrobenzoic acid); DTT, DL-dithiothreitol; EDTA, ethylenediamine tetraacetate; FTIR, Fourier transform infrared; IPTG, isopropyl- $\beta$ -D-thiogalactopyranoside; MALDI/TOF, matrix assisted laser desorption ionization/time of flight; OP, 1,10-phenanthroline; ORF, open reading frame; 4,7P, 4,7-phenanthroline;  $\Psi$ , pseudouridine; UV-CD, ultraviolet–circular dichroism.

From the comparison of the amino acid sequences, the few RNA- $\Psi$  synthetases identified so far have been partitioned into four families (10, 18). The proteins of the first three families (related to *E. coli* RluA, *E. coli* RsuA, and *E. coli* TruB, respectively) are site-specific RNA- $\Psi$  synthetases and exhibit conserved motifs, particularly a motif similar to that found in deoxycytidine deaminase (19) and deoxyuridine triphosphatase (20), with a strictly conserved aspartic acid. However, the similarity between the three families is limited to short motifs and it is likely that the common reaction catalyzed by these enzymes requires a very limited sequence. The sequence divergence between these proteins might be related to the recognition of different structural elements in RNA (18). The fourth group is related to *E. coli* TruA. This group of TruA-like enzymes is rather distant from the three other families. Pus1, previously referred to as Los2 (21), was originally discovered because it displayed amino acid sequence homology with the *E. coli* TruA, with the yeast Pus3 (previously referred to as Deg1) (22), and with a yeast ORF called Pus2 (previously referred to as Los3) (9) and therefore belongs to this family. The TruA-like proteins also exhibit a conserved sequence with a strictly conserved aspartic acid, likely involved in catalysis.

In the present work we demonstrate that the yeast tRNA- $\Psi$  synthetase Pus1 is a zinc metalloprotein. It is the first time that zinc is found to be associated to a RNA-pseudouridine synthetase.

## MATERIALS AND METHODS

**Enzymes and Chemicals.** 1,10-Phenanthroline (OP), spermidine, diethyl pyrocarbonate (DEP), 5,5'-dithio-bis(2-nitrobenzoic acid) (DTNB), iodoacetamide, disodium ethylenediaminetetraacetate (EDTA), bovine serum albumin (BSA), thrombin, and activated charcoal were purchased from Sigma Chemical Co. (St. Louis, MO). 4,7-Phenanthroline (4,7P) was from Aldrich (Milwaukee, WI), isopropyl- $\beta$ -D-thiogalactopyranoside (IPTG), DL-dithiothreitol (DTT), DL-dithioerythreitol (DTE), *MvaI* restriction endonuclease, and T7-RNA polymerase were from MBI fermentas (Vilnius, Lithuania), the nucleotide triphosphates were from Boehringer (Manheim, Germany), dodecyl-D-maltoside (DDM) was from Fluka (Buchs, Switzerland), Ni-NTA resin was from Qiagen (Hilden, Germany), the nitrocellulose filters were from Sartorius-GmbH (Germany), and [5- $^3$ H]UTP was from Amersham (UK). All other chemicals were from Sigma (St. Louis, MO) or Merck-Biochemicals (Darmstadt, Germany).

**Buffers.** The different buffers used in this work were the following: buffer A, 50 mM potassium phosphate (pH 8) containing 200 mM NaCl, 1 mM DTT, and 0.5 mg/mL dodecyl maltoside; buffer B, 20 mM Tris-HCl (pH 8.5) containing 10% glycerol, 1 mM DTT, 1 mM MgCl<sub>2</sub>, and 0.5 mg/mL dodecyl maltoside; buffer C, 20 mM Tris-HCl (pH 8) containing 3 mM MgCl<sub>2</sub>, 1 mM spermidine, 5 mM NaCl, 0.025% Tween-20, and 2 mM DTT; buffer D, 20 mM Tris-HCl (pH 8.5) containing 100 mM KCl, 1 mM DTT, 10% glycerol, and 0.1 mg/mL BSA; buffer E, 50 mM Tris-HCl (pH 8.5) containing 1 mM EDTA, 100 mM KCl, 1 mM DTT, and 0.5 mg/mL dodecyl maltoside; buffer F, 50 mM Tris-HCl (pH 8.5) containing 10% glycerol, 1 mM DTT, and 0.5 mg/mL dodecyl maltoside.

**Expression, Purification, and Characterization of Recombinant Pus1.** The *pus1* ORF, cloned into a pET vector (pET 8c), was a generous gift of G. Simos and Ed. Hurt (University of Heidelberg, Germany). Its gene product was a Pus1 protein bearing an extension (His)<sub>6</sub>-(Ser)<sub>2</sub> at the N terminus. This gene was under the control of the T7 polymerase promoter (9). Transformation was performed in *E. coli* BL21(DE3), which contained the T7 polymerase gene under the control of an IPTG-inducible promoter. Cells were grown at 37 °C in 15 L of minimal medium supplemented with 20  $\mu$ M ZnCl<sub>2</sub>, 1 mM MgSO<sub>4</sub>, and 100 mg/L ampicillin. When the optical density reached OD<sub>600</sub> = 0.7, the temperature was shifted to 25 °C and IPTG (0.5 mM final concentration) was added. The cells were collected by centrifugation at 4 °C (6000g for 5 min) and resuspended in buffer A supplemented by 0.1% Triton X-100. Cells were broken by sonication and the lysate was centrifuged (12000g for 15 min). The recombinant Pus1 fusion protein, present in the supernatant, was further purified using a Ni-NTA column, using buffer A supplemented with 150 mM imidazole to elute the bound proteins. After the Ni-NTA column, the eluted proteins were immediately filtered through a small column of Sephadex G-25 M (Pharmacia, Sweden), with a buffer B supplemented with 1 mM EDTA to remove free Ni<sup>2+</sup> ion. Recombinant Pus1 was further purified by anion exchange chromatography on a Mono Q HR5/5 prepacked column (Pharmacia, Sweden) equilibrated with buffer B. Elution was performed with a linear gradient of NaCl (from 0 to 300 mM). Under these conditions, nucleic acids (including tRNA) remain bound on the column. After this step, only one band is observed on SDS-PAGE (63 kDa) followed by silver staining. Since recombinant Pus1 tends to aggregate and to adsorb on dialysis membranes, the neutral detergent dodecyl-D-maltoside at a concentration of 0.5 mg/mL was added to all buffers and enzyme samples. Protein concentration was determined either by measuring the absorption at 280 nm, using an extinction coefficient  $\epsilon_{280}^{1\text{mg/mL}} = 0.75$ , as calculated from the amino acid composition of Pus1, or by using the Bradford assay (Bio-Rad) with BSA as a standard (23). The molecular mass of Pus1 was determined on a MALDI/TOF Voyager Elite Perspective BioSystems mass spectrometer (Framingham, MA). The dried droplet technique was used. Pus1 (5 pmol) was added to a saturated solution of synapinic acid in 30% acetonitrile and 0.1% trifluoroacetic acid (TFA). The mass spectrometer was calibrated using the MH<sup>+</sup> and (M + 2H<sup>+</sup>)/2 peaks of BSA (67 kDa). The His<sub>6</sub>-Pus1 construct did not contain any specific proteolytic cleavage site. However, the presence of thrombin cleavage sites in the N-terminal region of Pus1 (probably an Arg-Gly site, 19 amino acids after the His<sub>6</sub> tag) allowed the removal of a fragment including the His<sub>6</sub> Tag. Proteolysis was performed at 30 °C for 16 h, at a ratio of 5 NIH units of thrombin/mg of fusion protein. The His<sub>6</sub> tag containing fragment and the truncated Pus1 were separated using a Ni-NTA column as described above.

**Preparation of Tritiated tRNA Substrate.** Runoff T7-transcripts of the yeast tRNA<sup>Val</sup> gene were prepared from a plasmid given by B. Senger and F. Fasiolo (24). Plasmids were linearized in a reaction mixture containing 50 mM Tris-HCl (pH 7.5), 10 mM MgCl<sub>2</sub>, 100 mM NaCl, 1 mM DTE, 0.1 mg/mL bovine serum albumin, 0.25 mg/mL plasmid, and 250 units/mL *MvaI* for 3 h at 37 °C. The reaction was

stopped by phenol-chloroform treatment, and the linear plasmid was recovered by ethanol precipitation. Transcription was performed overnight at 37 °C, using 0.25 mg/mL linear plasmid in a buffer C supplemented with 1 mM each of ATP, CTP, and GTP, 0.05 mM UTP, and 500  $\mu$ Ci/mL of [5-<sup>3</sup>H]UTP (specific activity: 10 Ci/mmol). The reaction was initiated by the addition of 2000 U/mL T7-RNA polymerase. The resulting tRNA<sup>Val</sup> bearing uracil labeled on C5 with [<sup>3</sup>H] was purified by phenol-chloroform extraction, ethanol precipitation, and gel filtration on a microspin S-200 HR (Pharmacia, Sweden). The yield of tRNA substrate, lacking all of the modified nucleotides normally present in the fully matured yeast tRNA<sup>Val</sup>, was about 20 pmol (specific activity 85 Ci/mmol).

**Pseudouridine Formation Assay.** Pus1 activity was assayed by measuring the rate of [<sup>3</sup>H<sup>+</sup>] liberation from [5-<sup>3</sup>H]-uracil-containing yeast tRNA<sup>Val</sup>. This uracil isomerization test is based on a method initially described by Cortese et al. (17). The reaction mixture contained 100 mM Tris-HCl (pH 8), 10 mM MgSO<sub>4</sub>, 0.1 mM EDTA, 100 mM NH<sub>4</sub>OAc, 8 nM [5-<sup>3</sup>H] uracil-containing tRNA<sup>Val</sup> transcript, 0.5 mM DTT, and recombinant Pus1. Incubation was performed at 37 °C. At various time intervals, 20- $\mu$ L aliquots were withdrawn and the reaction was stopped by mixing the samples with 500  $\mu$ L of 0.1 M HCl containing 12% activated charcoal. Each sample was vigorously stirred and centrifuged at 10000g for 1 min. Radioactivity corresponding to free [<sup>3</sup>H<sup>+</sup>] present in the supernatant was evaluated in aliquots using a liquid scintillation counter. In our experimental conditions Pus1 is present in excess compared to tRNA. Thus, unless otherwise stated, the final concentrations of Pus1 and [5-<sup>3</sup>H]-uracil-containing tRNA<sup>Val</sup> transcript were 275 nM and 8 nM, respectively.

**tRNA Binding Assay.** Various concentrations of recombinant Pus1 were mixed at 20 °C with a fixed concentration of [<sup>3</sup>H]-uracil-labeled yeast tRNA<sup>Val</sup> transcript (50 pM) in buffer D (total volume of 0.1 mL). In these conditions Pus1 is in large excess compared to tRNA. After a 30-min incubation at 20 °C, each sample was slowly filtered through a nitrocellulose filter (0.45  $\mu$ m, Sartorius). Filters were washed with buffer D lacking BSA and then dried by infrared irradiation, and the radioactivity associated with the proteins adsorbed on the filter was measured using a liquid scintillation counter.

**Determination of Zinc Content in Pus1.** The molar amount of zinc in Pus1 (100- $\mu$ L solution at 5–20  $\mu$ M) was measured at 213.9 nm using a flame atomic absorption spectrophotometer (type Varian AA 755). To avoid metal contamination, all glasses and plastic wares to which the enzyme solution could be exposed were previously washed with 10 mM EDTA and rinsed with deionized water. Prior to the experiments, enzyme solutions were dialyzed overnight at 4 °C against buffer E. The zinc content of Pus1 was evaluated from a standard curve obtained with ZnCl<sub>2</sub> at different concentrations in the range 0–40  $\mu$ M. Three independent determinations were made for each sample.

**Chemical Modification of the His and Thiol Groups in Pus1.** The carbethoxylation of the histidine residues of recombinant Pus1 was carried out by incubating the protein (10  $\mu$ M) with a 1000-fold molar excess of diethylpyrocarbonate (DEP) in K phosphate buffer (pH 7) for 60 min at room temperature. The enzyme solution was then dialyzed

overnight at 4 °C against buffer E to eliminate the residual DEP.

Modification of the thiol groups of recombinant Pus1 was carried out by incubation of the enzyme (10  $\mu$ M) with iodoacetamide (10 mM in 100 mM Tris-HCl pH 8) for 60 min at room temperature. Excess iodoacetamide was eliminated by dialysis overnight at 4 °C against buffer E.

Quantification of the free cysteine residues of recombinant Pus1 was performed in the presence of 6 M guanidine hydrochloride. Titration was performed with DTNB (3 mM in 100 mM K phosphate buffer pH 7.3) and the number of free cysteine residues available in the denatured Pus1 (10  $\mu$ M) was estimated by spectrophotometry using a molar absorption coefficient of  $\epsilon_{412} = 13\,700\text{ M}^{-1}\text{ cm}^{-1}$  for the aromatic thiol product.

**Analytical Ultracentrifugation.** Centrifugation was performed at 20 °C in a Beckman Optima XLA ultracentrifuge using an AN60-titanium four-hole rotor and a cell with two-channel centerpieces (path length 12 mm). Prior to centrifugation, recombinant Pus1 samples were dialyzed overnight at 4 °C against buffer F. Measurements were performed at 60 000 rpm. Radial scans of absorbency at 280 nm were taken at 5-min intervals, the dialysis buffer being used as the reference. Data were analyzed using the programs SVEDBERG and SEDNTERP (25, 26). The partial specific volume of recombinant Pus1 was calculated to be 0.732 cm<sup>3</sup> g<sup>-1</sup> at 20 °C and the solvent density was 1.028.

**Circular Dichroism Spectra.** UV-CD spectra of recombinant Pus1 (0.15 mg/mL), previously dialyzed overnight against buffer F, were recorded using a Jobin-Yvon Mark VI high-sensitivity dichrograph equipped with a thermostatic cell holder. The CONTIN program (27) was used to estimate the protein secondary structure from the CD spectrum. The  $\alpha$  helix percentage was also calculated from the ellipticity at 222 nm (28).

**Infrared Spectra.** Attenuated total reflectance (ATR) FTIR spectra were measured with a Bruker IFS 66 spectrophotometer equipped with a 45°n ZnSe ATR attachment. The spectra shown are the average of 1000 scans. Spectra were corrected for the linear dependence of the absorption measured by ATR on the wavelength. The water signal was removed by the subtraction of a buffer spectrum. Analysis of the protein secondary structure composition was performed by deconvolution of the absorption spectrum, either as a sum of Gaussian components (29) or as a sum of spectra associated with different structures (30).

**Fluorescence Spectra.** Pus1 fluorescence spectra were recorded at 20 °C using a Perkin-Elmer LS50B spectrofluorimeter. The excitation wavelength was set at 295 nm (bandwidth 4 nm), and emission spectra were recorded between 310 and 400 nm (bandwidth 4 nm). The concentration of the samples was 0.1 mg/mL in buffer F. All spectra were corrected by the background signal obtained with the buffer alone.

## RESULTS

**Purification and Characterization of Pus1 Expressed in *E. coli*.** Homogeneous protein (7–10 mg) was routinely obtained from the purification procedure described in Materials and Methods. In the presence of the neutral detergent DDM, Pus1 behaved as a monomer and was not integrated into a micelle. The molecular mass of the recombinant

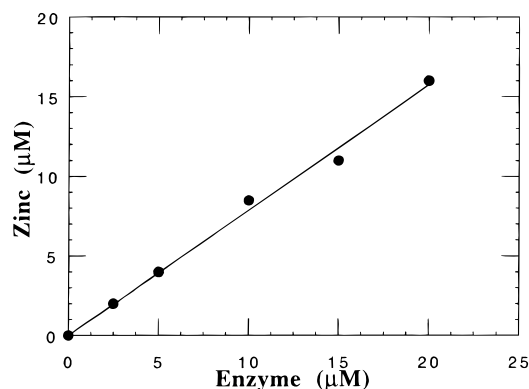


FIGURE 1: Determination of Pus1 zinc content. The enzyme was dialyzed overnight at 4 °C against buffer E. Enzyme concentrations were measured by absorbency at 280 nm, and zinc content determination was performed by flame atomic absorption spectroscopy as described in Materials and Methods.

protein (including the 6 histidines) determined by MALDI mass spectrometry was  $63.2 \pm 0.3$  kDa, in agreement with that deduced from the amino acid composition (63.14 kDa). The number of cysteine residues in the recombinant Pus1 was  $4.7 \pm 0.5$  free cysteines, in agreement with the cysteine content of Pus1 based on its amino acid composition (5 mol/mol of Pus1).

The specific activity of recombinant Pus1 was determined with the enzyme in excess compared to yeast tRNA<sup>Val</sup>. To ensure initial velocity conditions, we verified that [ $^3\text{H}$ ] liberation was proportional to incubation time or to tRNA concentration and was hyperbolic as a function of recombinant Pus1 concentration. The specific activities were calculated at enzyme concentrations corresponding to the first part of this hyperbolic curve (enzyme concentrations between 0 and 500 nM). DDM did not affect the activity of Pus1. The  $K_m$  of Pus1 for yeast tRNA<sup>Val</sup> was 425 nM. The catalytic constant  $k_{\text{cat}}$  of the enzyme, determined assuming that substrate was limiting, was  $0.4 \text{ min}^{-1}$ .

**Recombinant Pus1 Contains One Zinc Atom per Monomer.** The  $\text{Zn}^{2+}$  content of Pus1, as determined by flame atomic absorption spectroscopy, revealed the presence of  $0.75 \pm 0.05$  equiv of  $\text{Zn}^{2+}$ /polypeptide chain (Figure 1). Increasing the amount of  $\text{Zn}^{2+}$  ions in the cell growth media did not significantly increase Pus1 zinc content. Extensive dialysis of the purified recombinant Pus1 against solutions containing 1 mM EDTA did not significantly modify the zinc content of the enzyme. Moreover, the zinc atom remained tightly bound to Pus1 in the presence of 6 M urea (Table 1). A truncated Pus1 lacking an amino terminal fragment, including the His tag, contained 0.6–0.7 mol of zinc/mol of Pus1.

The precipitation of recombinant Pus1 at pH below 7.5 (result not shown) and its sensitivity to thiol reagents respectively suggests involvement of histidine and cysteine residues in enzyme structure and stability. The amino acid side chains which bind the zinc atom in Pus1 were determined by enzyme modification with diethylpyrocarbonate (DEP) or iodoacetamide, two reagents capable of covalently reacting with histidine and the cysteine residues, respectively. As shown in Table 1, incubation of Pus1 with DEP or iodoacetamide, followed by extensive dialysis against EDTA solution, led to the release of zinc atom, in parallel with enzyme activity loss. These results suggest that both histidine and cysteine residues are likely candidates for zinc

Table 1: Effect of EDTA, Urea, Iodoacetamide, and DEP on Zinc Content and Activity of Pus1<sup>a</sup>

treatment	zinc (mol of $\text{Zn}^{2+}$ /mol of Pus1)	activity (fmol of $\Psi$ /min)
control	$0.75 \pm 0.05$	$33 \pm 2$
EDTA	$0.73 \pm 0.05$	$32 \pm 2$
urea	$0.75 \pm 0.05$	$0 \pm 2$
DEP	$0.00 \pm 0.05$	$0 \pm 2$
iodoacetamide	$0.00 \pm 0.05$	$0 \pm 2$

<sup>a</sup> Activity measurement and zinc content determination were performed as described in Materials and Methods. In the case of EDTA or urea, Pus1 was dialyzed overnight against buffer E containing 1 mM EDTA or 6 M urea. In the case of iodoacetamide or DEP, Pus1 was directly incubated with an excess of each reagent and then dialyzed against buffer E to eliminate free iodoacetamide or DEP.

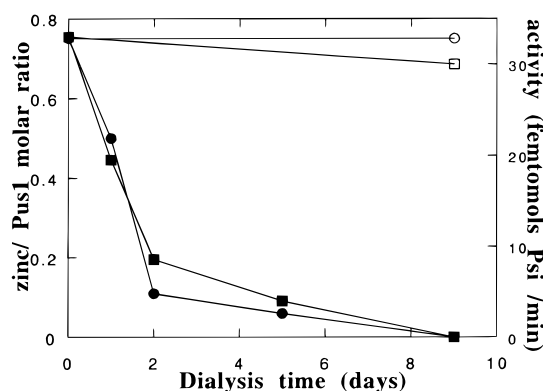


FIGURE 2: Influence of dialysis against 10 mM 1,10-phenanthroline (OP) on Pus1 activity and zinc content. Pus1 samples (6 μM, 1.5 mL) were dialyzed at 4 °C against buffer E, with (■, ●) or without (□, ○) 10 mM OP. At various times, aliquots were withdrawn for activity measurements (■, □) and zinc content determination (●, ○), as described in Materials and Methods.

binding. However, one cannot exclude that the modification of histidine and cysteine residues could cause drastic changes elsewhere in the protein that causes the zinc release.

**Zinc Removal by 1,10-Phenanthroline.** 1,10-Phenanthroline (OP) is a strong chelator for zinc ( $K_{\text{d}}(\text{Zn:OP}) = 4 \times 10^{-7}$  M at 25 °C, pH 7). To test the possibility of zinc removal by OP, a sample of Pus1 was dialyzed for several days against buffer F containing 10 mM chelator. Control experiments were performed under identical conditions in the absence of OP in the dialysis buffer. At various times, aliquots were withdrawn and extensively dialyzed against buffer lacking OP and both the enzymatic activity and the zinc content were measured. As shown in Figure 2, within 10 days,  $\text{Zn}^{2+}$  was progressively removed from Pus1. Removal of  $\text{Zn}^{2+}$  paralleled the enzyme activity loss (Figure 2). When Pus1 was dialyzed against buffer without OP,  $\text{Zn}^{2+}$  content was unchanged, while the enzyme lost only 15% of its activity. Since this aromatic compound might affect the pseudouridylation reaction as a consequence of its intercalation within the double-stranded nucleic acids (31, 32), OP was completely removed by dialysis prior to the residual activity measurements. Removal of OP from the enzyme was slow (3 days at 4 °C), suggesting a high affinity of chelating agent for the enzyme.

**Effects of 1,10-Phenanthroline and 4,7-Phenanthroline on Pus1 Activity.** The pseudouridylation activity of Pus1 was lost within 5 min in the presence of 40 mM OP, while the

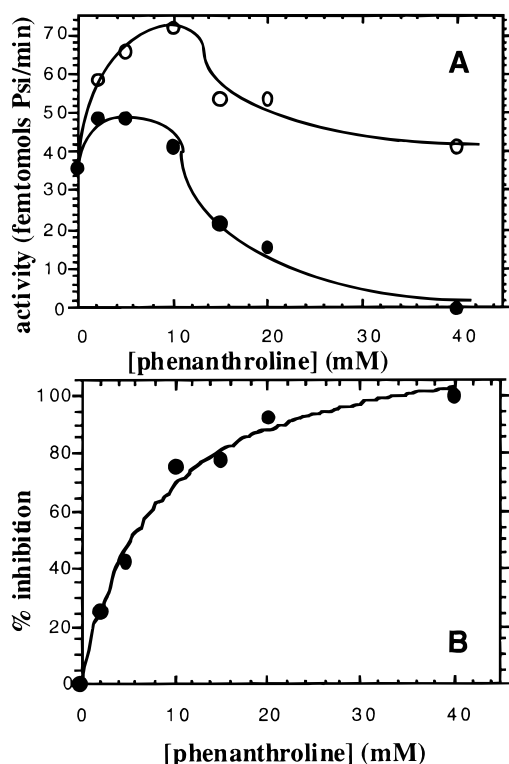


FIGURE 3: Effect of 1,10-phenanthroline and 4,7-phenanthroline on Pus1 activity. Part A: Pus1 was incubated with the chelating agent 1,10-phenanthroline (●) and nonchelating 4,7-phenanthroline (○) at various concentrations. Part B: Inhibition due to zinc chelation as a function of the concentration of phenanthroline. This inhibition curve, expressed as a percent of inhibition, represented the subtraction of the intercalation effect (4,7P) from the chelating effect (OP).

zinc content of Pus1 remained unchanged for more than 1 h of dialysis against 40 mM OP (result not shown). Those results suggest that enzyme inhibition by OP is due to in situ chelation of the zinc atom rather than removal of the metal. To distinguish between enzyme inhibition by OP and unrelated phenomena, such as OP intercalation in the tRNA substrate, the effects of increasing the concentration of OP (0 to 40 mM) were compared to those of its nonchelator isomer 4,7-phenanthroline (4,7P). As shown in Figure 3A, in the presence of OP and 4,7P at concentrations ranging from 1 to 10 mM, the activity of Pus1 was significantly increased. By contrast, above 10 mM OP, Pus1 activity was dramatically reduced, while in the presence of 4,7P, enzyme activity remained unchanged. Figure 3B shows the percentage of inhibition of Pus1 as a function of OP concentration. This inhibition curve represented the subtraction of the intercalation effect (4,7P) from the chelating effect (OP). This curve was analyzed assuming that OP, when bound to Pus1, totally abolished enzyme activity. An inhibition constant of 8 mM could be deduced for OP.

**Zinc-Depleted Pus1 Is Unable To Bind tRNA.** As shown in Figure 4, Zn-depleted Pus1 was unable to bind tRNA, whereas the native enzyme could form a reversible michaelian complex with tRNA<sup>Val</sup> (apparent  $K_d$  of 10 nM in buffer D at 20 °C). These results strongly suggest a structural role for the zinc atom in Pus1.

**Zinc-Depleted Pus1 Can Bind Zinc Again.** Following prolonged dialysis against buffer E containing 10  $\mu$ M ZnCl<sub>2</sub>, the inactive zinc-depleted enzyme was shown to recover 25%

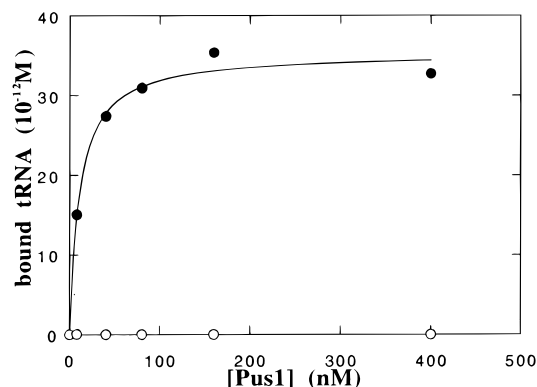


FIGURE 4: Binding of yeast tRNA<sup>Val</sup> by native (●) or zinc-depleted (○) Pus1 measured by filter binding assay. Pus1 (0–400 nM) and tRNA ( $50 \times 10^{-12}$  M) were incubated for 30 min at 20 °C in 20 mM Tris-HCl pH 8.5 buffer containing 10% glycerol, 100 mM KCl, 1 mM DTT, and 0.1 mg/mL BSA.

Table 2: Reinsertion of Zinc in the Apoenzyme Pus1<sup>a</sup>

	native	zinc-depleted Pus1	zinc-reconstituted Pus1
zinc content (mol of Zn <sup>2+</sup> /mol of Pus1)	0.75 $\pm$ 0.05	0.00 $\pm$ 0.05	0.20 $\pm$ 0.05
activity (fmols of $\Psi$ /min)	33 $\pm$ 2	0 $\pm$ 2	8 $\pm$ 2

<sup>a</sup> Zinc-depleted enzyme which had been obtained by dialysis of native Pus1 against buffer E containing 10 mM OP was reconstituted by further dialyzing the apoenzyme against buffer E containing 10  $\mu$ M ZnCl<sub>2</sub>. After the removal of free Zn<sup>2+</sup> by dialysis against buffer E containing 1 mM EDTA, activity measurements and the zinc content determination were performed as described in Materials and Methods.

Table 3: Effect of Zinc Depletion on Pus1 Conformation<sup>a</sup>

	native Pus1	zinc-depleted Pus1
$S_{20,w}$ (S)	3.15 $\pm$ 0.05	2.70 $\pm$ 0.03
$R_s$ (Å)	47	54
length, $l$ (Å)	100	160
diameter, $d$ (Å)	38	31
$l/d$	2.6	5.1
zinc (mol of Zn <sup>2+</sup> /mol of Pus1)	0.75 $\pm$ 0.05	0.00 $\pm$ 0.05

<sup>a</sup> Analytical ultracentrifugation experiments of native and zinc-depleted enzyme were performed at 20 °C. Zinc-depleted Pus1 was treated for 10 days against buffer E containing 10 mM OP. Native Pus1 was treated in the same conditions without OP. Determination of the zinc content was performed as described in Materials and Methods. Length ( $l$ ) and diameter ( $d$ ) of Pus1 (in a cylindrical model) and its stokes radius ( $R_s$ ) were evaluated using the program Svedberg and Sednterp from J. Philo (Philo 1994 and Laue et al. 1992).

of bound zinc, along with 25% of the pseudouridylation activity (Table 2).

**Zinc Removal Triggers a Tridimensional Conformational Change in Pus1.** The effect of zinc removal on enzyme conformation was investigated. Zinc depletion results in the precipitation of 80% of Pus1. In the control Pus1, only 15% of the enzyme was precipitated. Aggregates were removed by centrifugation (12000g, 60 min) prior to analysis.

Sedimentation velocity experiments have demonstrated that zinc-containing Pus1 has a higher  $S_{20,w}$  than the zinc-depleted enzyme, suggesting that a global conformational change had occurred in zinc-depleted Pus1 (Table 3). Zinc-depleted Pus1 ( $S_{20,w}$  = 2.7 S) seems more extended than native Pus1 ( $S_{20,w}$  = 3.15 S). These results account for a

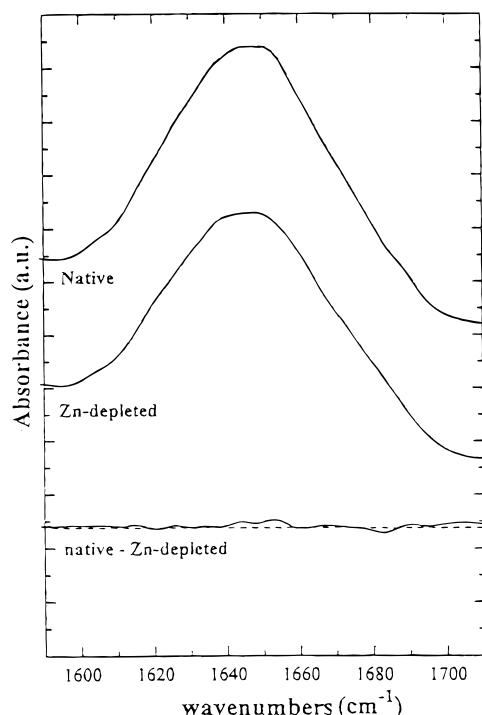


FIGURE 5: FTIR spectra of native or zinc-depleted Pus1. Spectra were measured at 20 °C at a protein concentration of 5 mg/mL. The spectra shown are the average of 1000 scans and were corrected for the linear dependence of the absorption measured by ATR (attenuated total reflectance) on the wavelength, resulting from the variation in the penetration of the sample by the evanescent wave. The water bending mode absorption in the vicinity of the amide bands was removed by the subtraction of a buffer spectrum.

Stokes radius ( $R_s$ ) of 47 Å for the native protein and 54 Å for the zinc-depleted protein. The  $R_s$  value of 54 Å for zinc-depleted Pus1 is abnormally high for a 63-kDa protein ( $R_s$  = 52 Å for bovine liver catalase, molecular mass = 232 kDa). However, this abnormal  $R_s$  could not be accounted for by an oligomerization of the apoenzyme, because the sedimentation coefficient of zinc-depleted enzyme was smaller than that of the native enzyme. Thus, the increase of the Stokes radius of zinc-depleted Pus1 is most probably due to the partial unfolding of the protein. The content in secondary structural elements of the native or zinc-depleted Pus1 was measured by infrared spectroscopy (FTIR) and circular dichroism (UV-CD). Figure 5 shows the FTIR spectra of the Pus1 protein, either native or Zn-depleted. The difference between these spectra was small (less than 2%), thus indicating that, if any, changes in the secondary structure of Pus1 upon  $Zn^{2+}$  depletion might affect only few amino acids (at most 10 of the 552 amino acids). The content in secondary structural elements was deduced from the decomposition of the FTIR spectra as summarized in Table 4. Although the accuracy of such decomposition is quite low, it must be noted that UV-CD experiments gave very similar results (Table 4). In good agreement with the FTIR experiments, no change in the  $\alpha$ -helical content of the Pus1 protein was observed in UV-CD upon  $Zn^{2+}$  depletion. Differences in CD spectra (Figure 6) were observed around the 190-nm band and might reflect Pus1 aggregation instead of a decrease in  $\beta$  sheet content. Fluorescence spectra of Pus1 indicate that the tryptophan fluorescence emission band slightly red shifted (2 nm) upon zinc depletion (Figure

Table 4: Effect of Zinc Depletion on Pus1 Secondary Structure<sup>a</sup>

expt.	secondary structure	% area (wave no.)	
		native	zinc-depleted
FTIR	$\alpha$ helix	35 (1652)	32 (1653)
	$\beta$ sheet	19 (1673, 1630, 1622)	25 (1673, 1624)
	$\beta$ turn	1 (1686)	0.6 (1680)
	other structures	44 (1640)	42 (1639)
expt	secondary structure	% structure	
		native	zinc-depleted
UV-CD	$\alpha$ helix	30	33
	$\beta$ sheet	24	10
	other structures	46	58
zinc (mol of $Zn^{2+}$ /mol of Pus1)		$0.75 \pm 0.05$	$0.00 \pm 0.05$

<sup>a</sup> Zinc-depleted Pus1 was treated for 10 days against buffer E containing 10 mM OP. Native Pus1 was treated in the same conditions without OP. Determination of the zinc content was performed as described in Materials and Methods. Secondary structure elements of native or zinc-depleted Pus1 were deduced from FTIR and circular dichroism experiments. For FTIR experiments, the table shows Gaussian peaks deconvolved from the amide I band together with their structural assignments and relative areas. For circular dichroism experiments, secondary structures were estimated from the CD spectra by using Dr. Provencher's program CONTIN.

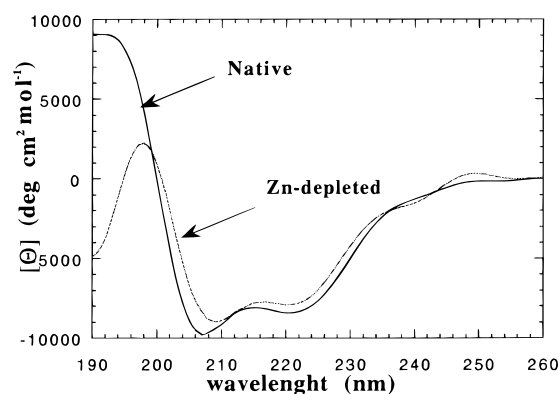


FIGURE 6: CD spectra of native or zinc-depleted Pus1. Circular dichroism spectra were recorded in the far-UV region (260–190 nm) at 20 °C and at a protein concentration of 0.15 mg/mL. CD was expressed as the mean residue ellipticity  $[\Theta]_r$ .

7). This result suggests a small change of conformation around one of the four tryptophan residues of Pus1.

## DISCUSSION

*Pus1 Is a New Zinc Metalloenzyme.* Yeast tRNA- $\Psi$  synthetase Pus1, as overexpressed and purified from *E. coli*, is a 63.2-kDa monomeric protein containing an average 0.8 mol of bound  $Zn^{2+}$ /polypeptide chain. This zinc atom is tightly bound since it could not be removed, neither by prolonged dialysis against EDTA nor by treatment with 6 M urea. Therefore it is likely that the zinc atom was not released from the enzyme in the course of the purification procedure. Quantitative removal of the zinc atom from Pus1 was achieved after prolonged dialysis for more than a week against OP, a strong chelator of zinc. The reason why OP could remove  $Zn^{2+}$  from native Pus1 while EDTA could not might be related to the type of coordination needed to chelate  $Zn^{2+}$ . Indeed, EDTA needs at least four free ligands to coordinate  $Zn^{2+}$  while OP is a bidentate chelating agent. It is also possible that tightly bound  $Zn^{2+}$  in the protein tridimensional structure is not accessible to EDTA (a charged

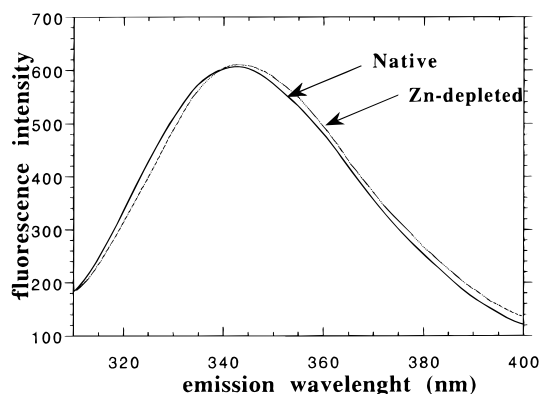


FIGURE 7: Fluorescence spectra of native or zinc-depleted Pus1. Spectra were recorded at 20 °C. The excitation wavelength was set at 295 nm (bandwidth 4 nm), and emission spectra were recorded between 310 and 400 nm (bandwidth 4 nm). The concentration of the samples was 0.1 mg/mL in buffer F. All spectra were corrected by the background signal obtained with the buffer alone.

molecule), while the OP (a neutral aromatic molecule) can access the bound  $\text{Zn}^{2+}$ . Identical observations have already been reported for several other zinc metalloproteins, including the *E. coli* methionyl-tRNA synthetase (33) and *E. coli* tRNA-guanine transglycosylase (34). A truncated Pus1, lacking the His<sub>6</sub> Tag, was shown to contain 0.6–0.7 mol of zinc/mol of protein, demonstrating that the His<sub>6</sub> Tag was not responsible for tight zinc binding.

**Zinc Removal Inactivates Yeast Pus1.** The removal of  $\text{Zn}^{2+}$  by prolonged dialysis against OP and the subsequent removal of the chelator itself led to a complete inhibition of the pseudouridylation reaction, similar to the zinc-containing aminoacyl-tRNA synthetases (35–37) and to tRNA-guanine transglycosylase (34). For Pus1, as for isoleucine-tRNA synthetase (35) and *E. coli* tRNA-guanine transglycosylase (34), inhibition results from the loss of tRNA binding capability of the zinc-depleted enzyme. This contrasts with *E. coli* methionyl- and glutamyl-tRNA synthetases (35, 36), where zinc was proposed to be necessary for the correct positioning of the 3' end of the acceptor stem of tRNA during amino acid transfer, rather than for the binding of the whole tRNA macromolecule.

**How Does 1,10-Phenanthroline Interact with Pus1 and tRNA?** Pus1 was inactivated by more than 99% within 5 min in the presence of 40 mM OP. This contrasts with the slow removal of the zinc by OP from the protein. Thus, the enzyme became inactivated, although zinc was still present in the holoenzyme. Inhibition of Pus1 by OP can be explained by a two-step model: OP would quickly bind to the enzyme to form a Pus1- $\text{Zn}^{2+}$ -OP ternary complex in which the pseudouridylation process would be impaired, probably because of steric hindrance. Upon dialysis, the chelating agent would slowly dissociate as a complex with zinc. In this model, zinc never appears as a free ion and therefore explains why EDTA cannot remove this metal. The inhibition constant  $K_i$  of Pus1 by OP was estimated to be 8 mM at 37 °C. This  $K_i$  value, which is 20 times higher than that of methionyl-tRNA synthetase ( $K_i = 0.4$  mM) (33), contrasts with the inhibition of horse liver lactate dehydrogenase (LADH) by OP, where a  $K_d$  of 33  $\mu\text{M}$  was measured (38).

Measurement of Pus1 activity as a function of the concentration of OP or 4,7P revealed that in the range 0–10

mM, either molecule was capable of promoting a significant activation of the pseudouridylation reaction. Above 10 mM, Pus1 activity in the presence of 4,7P decreased and became comparable to the control without phenanthroline, while in the presence of OP, enzyme activity was progressively inhibited. For example, at 40 mM 4,7P or OP, the residual Pus1 activity was approximately 100% and less than 1% of the control without phenanthroline, respectively. Since either molecule is capable of intercalating into double-stranded regions of RNA, one hypothesis is that, at low concentration, the fixation of OP or 4,7P to RNA makes the target uridine-27 in tRNA<sup>Val</sup> more accessible to Pus1. Above 10 mM, the binding of either agent to additional sites on the tRNA substrate might induce tridimensional changes in the structure that no longer lead to Pus1 activation. In turn, inhibition of Pus1 by OP at concentrations superior to 10 mM is likely to be due to the in situ zinc chelation.

**Structural Rather Than Catalytic Role For The Zinc.** As a consequence of  $\text{Zn}^{2+}$  removal, the sedimentation constant of Pus1 was lowered, while the major part of the zinc depleted-enzyme was found precipitated. These observations argue in favor of a conformational change in the 3-D structure of the enzyme, while CD, FTIR, and fluorescence measurements indicate only subtle changes in the internal protein organization. These results are consistent with a structural role for zinc in Pus1. One possibility is that zinc could maintain the association between domains, structurally organized around the coordinated metal ion and important for global protein structure integrity. Destruction of this “core” would induce a more opened structure, without affecting secondary structure elements. This situation has been observed in *E. coli* tRNA-guanine transglycosylase, where the metal coordination keeps the zinc subdomain tightly packed against the ( $\beta/\alpha$ ) barrel, as a “bridge zinc ion” and therefore plays an essential role for the structural integrity of the protein (39). Precipitation of  $\text{Zn}^{2+}$ -depleted enzyme could result from exposition of hydrophobic regions upon zinc removal, inducing protein-protein interactions. Partial solubilization of  $\text{Zn}^{2+}$ -depleted enzyme in the presence of the neutral detergent dodecyl-D-maltoside might imply that the detergent partially prevents interactions of the exposed hydrophobic surfaces. The less compact structure resulting from zinc depletion would be responsible for the loss of tRNA binding capability of the yeast Pus1. Upon prolonged dialysis against 10  $\mu\text{M}$   $\text{ZnCl}_2$ , zinc-depleted Pus1 was shown to recover 25% of bound zinc, along with 25% of pseudouridylation activity. It is likely that the remaining 75% of zinc-depleted enzyme was related to the precipitation of the enzyme during zinc depletion.

**Amino Acids Involved in Zinc Binding.** The naturally occurring zinc ligands generally encountered in proteins are the carboxylates of aspartate or glutamate, the sulfur atom of cysteine, the imidazole of histidine, and water molecules. When bound to proteins, the  $\text{Zn}^{2+}$  coordination number is usually four. Modification of cysteine and histidine residues with iodoacetamide or diethylpyrocarbonate led to an inactive and zinc-depleted Pus1. No less than 9 histidines (not including the 6 histidines from the Tag  $\text{NH}_2$  terminal) and 5 cysteines are found in Pus1. It is striking that none of the zinc binding consensus generally found in nucleic acid binding proteins described so far is present in the Pus1 sequence. However, inspection of this amino acid sequence

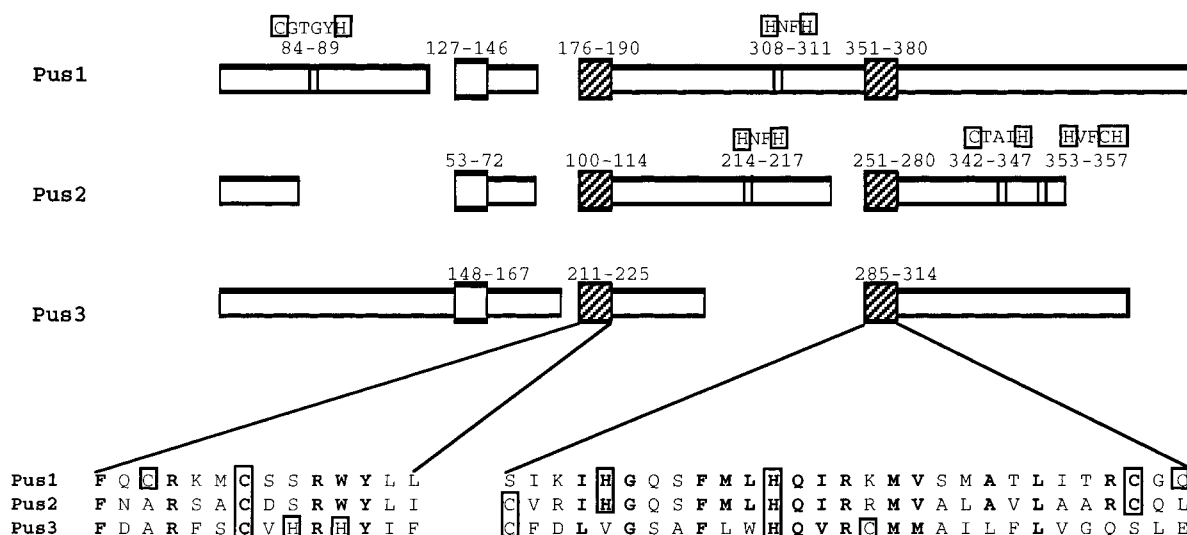


FIGURE 8: Alignment of the primary structures of Pus1, Pus2, and Pus3 around putative zinc-binding cysteines and histidines. Pus3 catalyzes the formation of  $\Psi$  at the positions 38/39 and the Pus2 function is unknown. Hatched boxes are conserved regions and bold-face characters are conserved amino acids. Histidine and cysteine residues are framed. The last motif is called cysteine/histidine box and is also found conserved in some DNA-directed RNA polymerases.

reveals the existence of several potential zinc binding motifs: **CX<sub>3</sub>C**, **HX<sub>2</sub>H**, **CX<sub>4</sub>H**, and a cysteines/histidines box **HX<sub>6</sub>HX<sub>14</sub>CXC** (with X = any amino acid, **H** = histidine, and **C** = cysteine). Moreover, multiple alignments of the amino acid sequence of Pus1 with the sequences of yeast tRNA-pseudouridine synthetases Pus2 and Pus3 constructed with the MACAW program (40) reveal three highly conserved regions (Figure 8). One of these is the cysteine/histidine box, also found in some zinc-containing DNA-directed RNA polymerase (archae bacteria and eukaryotes) (41). Another is the **CX<sub>3</sub>C** motif, including a strictly conserved cysteine (underlined). The strictly conserved **HNFH** found in Pus1 and Pus2 (but not in Pus3) is also a likely candidate for zinc binding. These motifs might represent signature sequences for metal binding. However, these potential zinc binding motifs found in Pus1 are not present in TruA, although this protein shares similarities with Pus1.

To date, Pus1 is the first example of zinc tRNA-pseudouridine synthetase. It may well be that, like for aminoacyl-tRNA synthetases, not all of the tRNA-pseudouridine synthetases contain zinc. The presence of a zinc atom in other members of this family will be investigated.

## ACKNOWLEDGMENT

We are particularly indebted to Drs. M. Ries and A. Ducruix (Gif-sur-Yvette) for many fruitful discussions and for suggesting the presence of zinc atom in Pus1. We thank Dr. G. Simos and Professor E. Hurt for providing us with the His<sub>6</sub>-Pus1 plasmid and Dr. F. Fasiolo for the plasmid containing the yeast tRNA<sup>Val</sup> gene. We are also grateful to C. Lazennec for technical assistance in flame atomic absorption spectroscopy, to Dr. S. Blanquet for the authorization to use these facilities (Ecole Polytechnique, Palaiseau), to G. Batelier (CNRS, Gif-sur-Yvette) for his help in performing the ultracentrifugation experiments, to J. Philo for making the computer programs available on the RASMB server, to Drs. F. Sourgen, M. Monnot, and S. Fermandjian (IGR,

Villejuif) for their help in performing the circular dichroism spectra, to Dr. Y. Gaudin (CNRS, Gif-sur-Yvette) for fluorescence spectra, to J. P. Lecaer (Ecole Supérieure de Physique et Chimie de la ville de Paris) for mass determination, and to M. Mehl for culture media preparation.

## REFERENCES

- Grosjean, H., Sprinzl, M., and Steinberg, S. (1995) *Biochimie* 77, 139–141.
- Sprinzl, M., Steegborn, C., Hubel, F., and Steinberg, S. (1996) *Nucleic Acids Res.* 24, 68–72.
- Reddy, R. (1990) *Methods Enzymol.* 180, 521–532.
- Szkukalek, A., Myslinski, E., Mouglin, A., Luhrmann, R., and Branlant, C. (1995) *Biochimie* 77, 16–21.
- Gu, J., Patton, J. R., Shimba, S., and Reddy, R. (1996) *RNA* 2, 909–918.
- Ofengand, J., and Bakin, A. (1997) *J. Mol. Biol.* 266, 246–268.
- Samuelsson, T., and Olsson, M. (1990) *J. Biol. Chem.* 265, 8782–8787.
- Becker, H., Motorin, Y., Planta, R. J., and Grosjean, H. (1997) *Nucleic Acids Res.* (1998) 25, 4493–4499.
- Simos, G., Tekotte, H., Grosjean, H., Segref, A., Sharma, K., Tollervey, D., and Hurt, E. C. (1996) *EMBO J.* 15, 2270–2284.
- Lecoite, F., Simos, G., Sauer, H., Hurt, E. C., Motorin, Y., and Grosjean, H. (1997) *J. Biol. Chem.* (1998) 273, 1316–1323.
- Patton, J. R. (1993) *Biochem. J.* 290, 595–600.
- Patton, J. R., Jacobson, M. R., and Pederson, T. (1994) *Proc. Natl. Acad. Sci. U.S.A.* 91, 3324–3328.
- Kammen, H. O., Marvel, C. C., Hardy, L., and Penhoet, E. E. (1988) *J. Biol. Chem.* 263, 2255–2263.
- Nurse, K., Wrzesinski, J., Bakin, A., Lane, B. G., and Ofengand, J. (1995) *RNA* 1, 102–112.
- Wrzesinski, J., Nurse, K., Bakin, A., Lane, B. G., and Ofengand, J. (1995) *RNA* 1, 437–448.
- Wrzesinski, J., Bakin, A., Nurse, K., Lane, B. G., and Ofengand, J. (1995) *Biochemistry* 34, 8904–8913.
- Cortese, R., Kammen, H. O., Spengler, S. J., and Ames, B. N. (1974) *J. Biol. Chem.* 249, 1103–1108.
- Koonin, E. V. (1996) *Nucleic Acids Res.* 24, 2411–2415.
- Taylor, A. F., and Weiss, B. (1982) *J. Bacteriol.* 151, 351–357.
- El-Hajj, H. H., Zhang, H., and Weiss, B. (1988) *J. Bacteriol.* 170, 1069–1075.



21. Sharma, K., Fabre, E., Tekotte, H., Hurt, E. C., and Tollervey, D. (1996) *Mol. Cell Biol.* 16, 294–301.
22. Carbone, M. L., Solinas, M., Sora, S., and Panzeri, L. (1991) *Curr. Genet.* 19, 1–8.
23. Bradford, M. M. (1976) *Anal. Biochem.* 72, 248–254.
24. Senger, B., Despons, L., Walter, P., and Fasiolo, F. (1992) *Proc. Natl. Acad. Sci. U.S.A.* 89, 10768–10771.
25. Philo, J. S. (1994) in *Modern Analytical Ultracentrifugation* (Schuster, T. M., and Laue, T. M., Eds.) pp 156–170, Birkhäuser, Boston.
26. Laue, T. M., Shah, B. D., Ridgeway, T. M., and Pelletier, S. (1992) in *Analytical Ultracentrifugation in Biochemistry and Polymer Science* (Harding, S. E., Rowe, A. J., and Horton, J. C., Eds.) pp 90–125, Redwood Press, Melksham, Wiltshire.
27. Provencher, S. W. (1982) *Comput. Phys. Commun.* 27, 229–242.
28. Zhong, L., and Johnson, C. W., Jr. (1992) *Proc. Natl. Acad. Sci. U.S.A.* 89, 4462–4465.
29. Byler, D. M., and Susi, H. (1986) *Biopolymers* 25, 469–487.
30. Kalnin, N. N., Baikalov, I. A., and Venyaminou, S. Y. (1990) *Biopolymers* 30, 1273–1280.
31. Veal, J. M., and Rill, R. L. (1991) *Biochemistry* 30, 1132–1140.
32. Auxilien, S., Crain, P. F., Trewyn, R. W., and Grosjean, H. (1996) *J. Mol. Biol.* 262, 437–458.
33. Mayaux, J. F., Kalogerakos, T., Brito, K. K., and Blanquet, S. (1982) *Eur. J. Biochem.* 28, 41–46.
34. Chong, S., Curnov, A. W., Huston, T. J., and Garcia, G. A. (1995) *Biochemistry* 34, 3694–3701.
35. Fourmy, D., Mechulam, Y., and Blanquet, S. (1995) *Biochemistry* 34, 15681–15688.
36. Liu, J., Lin, S. X., Blochet, J. E., Pezolet, M., and Lapointe, J. (1993) *Biochemistry* 32, 11390–11396.
37. Glassfeld, E., and Schimmel, P. (1997) *Biochemistry* 36, 6739–6744.
38. Drum, D. E., and Vallee, B. L. (1970) *Biochemistry* 9, 4078–4086.
39. Romier, C., Reuter, K., Suck, D., and Ficner, R. (1996) *EMBO J.* 15, 2850–2857.
40. Shuler, G. D., Altshul, S. F., and Lipman, D. J. (1991) *Proteins: Struct., Funct., Genet.* 9, 180–190.
41. Berghoffer, B., Krockel, L., Kortner, C., Truss, M., Schallenberg, J., and Klein, A. (1988) *Nucleic Acids Res.* 16, 8113–8128.

BI9726710